

Magnetization steps in $\text{Sn}_{1-x}\text{Eu}_x\text{Te}$: Eu-Eu exchange and Eu distribution

This article has been downloaded from IOPscience. Please scroll down to see the full text article.

2000 J. Phys.: Condens. Matter 12 3711

(<http://iopscience.iop.org/0953-8984/12/15/317>)

View [the table of contents for this issue](#), or go to the [journal homepage](#) for more

Download details:

IP Address: 171.66.16.221

The article was downloaded on 16/05/2010 at 04:49

Please note that [terms and conditions apply](#).

Magnetization steps in $\text{Sn}_{1-x}\text{Eu}_x\text{Te}$: Eu–Eu exchange and Eu distribution

X Gratens[†], E ter Haar[†], V Bindilatti[†], N F Oliveira Jr[†], Y Shapira[‡],
M T Liu[‡], Z Golacki[§], S Charar^{||} and A Errebbahi^{||}

[†] Instituto de Física, Universidade de São Paulo, CP 66318, CEP 05315-970 São Paulo, SP, Brazil

[‡] Department of Physics and Astronomy, Tufts University, Medford, MA 02155, USA

[§] Institute of Physics, Polish Academy of Sciences, PL 02-668 Warsaw, Poland

^{||} Groupe d'Etude des Semiconducteurs URA 357, Université Montpellier II, Place Eugene Bataillon, 34095 Montpellier Cédex 5, France

E-mail: vbindilatti@if.usp.br

Received 26 November 1999

Abstract. The magnetization of $\text{Sn}_{1-x}\text{Eu}_x\text{Te}$, with $x = 0.011$ and 0.042 , was measured at 20 mK in magnetic fields up to 90 kOe. Magnetization steps (MSTs) from pairs and triplets were observed. The MSTs give $J/k_B = -0.311 \pm 0.006$ K for the dominant Eu–Eu exchange constant. Comparisons of the magnetization curves with numerical simulations indicate that, instead of being distributed randomly, the Eu ions tend to bunch together. A phenomenological approach which uses the concept of a local Eu concentration x_L is quite successful in describing the data for these two samples.

1. Introduction

The dominant Eu–Eu exchange constant J for IV–VI dilute magnetic semiconductors (DMS) containing europium has been the subject of several experimental studies. In the early works the temperature variation of the low-field susceptibility and high-field magnetization at 4.2 K were used to estimate J in various IV–VI DMS, including $\text{Sn}_{1-x}\text{Eu}_x\text{Te}$ [1–3]. For the series $\text{Pb}_{1-x}\text{Eu}_x\text{X}$ ($X = \text{S}, \text{Se}, \text{Te}$), much more accurate values of J were obtained later from measurements of magnetization steps (MSTs) at 20 mK [4–6]. The largest Eu–Eu exchange constant in IV–VI DMS, which is between nearest neighbours (NNs), was found to be antiferromagnetic (AF), with a typical value of -0.2 K. This value is two orders of magnitude smaller than the dominant Mn–Mn exchange constant in II–VI DMS [7].

In addition to exchange constants, measurements of MSTs also give information about the distribution of the magnetic ions in the crystal. Specifically, the data indicate whether the magnetic ions (e.g., Eu^{2+} or Mn^{2+}) are randomly distributed over the cation sites, or whether they tend to bunch together. (We use the term ‘bunch together’ instead of ‘cluster’ because in this paper ‘cluster’ refers to a small number of neighbouring spins which form a group, e.g., a ‘pair’ consisting of two spins, or a ‘triplet’ of three spins.) In melt-grown II–VI DMS containing Mn the MST data were always consistent with a random distribution [7], but a tendency of the Eu ions to bunch together was clearly observed for Bridgman-grown $\text{Pb}_{1-x}\text{Eu}_x\text{Te}$ [5]. For $\text{Sn}_{1-x}\text{Eu}_x\text{Te}$ the Eu distribution is a significant issue because precipitates of EuTe were observed in samples with $x > 0.014$ [3, 8]. This finding indicates a tendency of the Eu ions to bunch together even in samples with relatively low x .

Europium enters SnTe as Eu^{2+} [9], which is an S-state ion with spin 7/2 and very low anisotropy. EPR data [10, 11] gave a g -factor of 1.99, and showed no dependence on magnetic field orientation and no detectable crystal-field splitting. The present work on the MSTs in $\text{Sn}_{1-x}\text{Eu}_x\text{Te}$ yielded an accurate value for the dominant Eu–Eu exchange constant for this material. The data also gave a quantitative measure of the tendency of the Eu ions to bunch together in our samples. The theory of the MSTs, and the method of analysing MST data on IV–VI DMS, were discussed in detail previously [4–6]. Much of the analysis in the present paper is similar to those in references [4] and [5].

2. Experimental procedure

The two $\text{Sn}_{1-x}\text{Eu}_x\text{Te}$ samples used in the MST measurements were grown by the Bridgman method. Following the growth, the sample with the higher Eu concentration was annealed at 700 °C for one week. The annealing took place in an evacuated quartz ampoule containing a small amount of Sn. After annealing, the sample was cooled quickly to room temperature. Each sample had the shape of a rectangular parallelepiped with linear dimensions of several mm.

The Eu concentration was determined from magnetization data at 2 K, measured in magnetic fields H up to 55 kOe using a SQUID magnetometer. These data, after a small correction for the lattice diamagnetism, were fitted to an effective Brillouin function [12] whose saturation value yielded x . The results were $x = 0.011 \pm 0.001$ for one sample, and $x = 0.042 \pm 0.002$ for the other. Fits of the low-field susceptibility data to the Curie–Weiss law were also made. The results for x , from the Curie constants, were 0.010 ± 0.005 and 0.041 ± 0.002 . The corresponding Curie–Weiss temperatures were $\theta = -0.7 \pm 0.2$ K and $\theta = -2.0 \pm 0.5$ K.

Microprobe measurements on one of the two large faces of the lower- x sample gave an average Eu concentration $x = 0.010$. Each microprobe measurement probed a ‘spot’ with a diameter of 1 μm , to a depth of about 1 μm . The Eu concentrations from the 52 spots which were measured for this sample were all within 10% of the average value quoted above. The microprobe measurement was made only on a portion of the higher- x sample (the sample broke after the MST data were taken). The results for 27 spots gave an average concentration $x = 0.034$, and showed deviations up to 30% from this average value. The values obtained from the magnetic data are the more accurate values since they refer to the overall Eu concentration x .

The temperature variation of the low-field susceptibility showed a normal paramagnetic behaviour for both samples, with a smooth monotonic variation near the Néel temperature of EuTe, $T_N \cong 10$ K. There was no evidence of any EuTe precipitates, which would have given rise to a cusp near 10 K [8]. (The susceptibility of other samples which we made measurements on did show the cusp from EuTe precipitates. They were not used in the MST experiments.) X-ray powder patterns for pieces adjacent to the two samples used in the MST experiments confirmed their rock-salt crystal structure and gave a lattice parameter of 6.32 Å for both samples. Furthermore, no evidence of EuTe precipitates was detected in the x-ray spectra. It was therefore concluded that although there is a tendency for EuTe precipitates to form, as reported earlier [3, 8], the specific two samples which were used in the MST measurements contained no detectable EuTe precipitates.

The magnetization data which show the MSTs were obtained at 20 mK. The experimental details have been described previously. A capacitance force magnetometer [13] operating in a plastic dilution refrigerator [14] and a 90 kOe superconducting magnet were used. The use of a dilution refrigerator completely made of plastic minimizes the eddy current heating during the field sweeps.

3. Results and discussion

Figure 1 shows the 20 mK magnetization of the two samples plotted as a function of the applied field H . The magnetization M is normalized to the value M_{max} at the highest field, which is very close to the saturation magnetization M_0 . The results include a small correction for lattice diamagnetism. The patterns exhibited in figure 1 are typical for the case where one antiferromagnetic exchange constant is much larger than all other exchange constants. The relevant contributions to the magnetization in this case have been described in reference [5] (see also figures 3 and 4 in reference [4]).

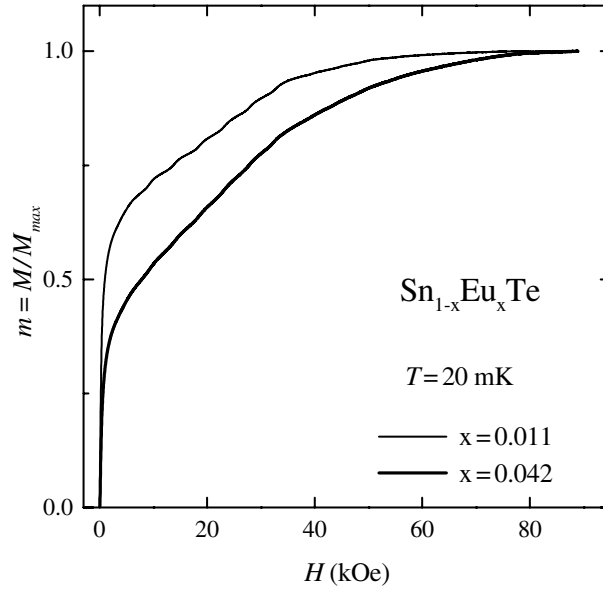


Figure 1. Magnetization curves for $x = 0.011$ and 0.042 , measured at 20 mK and corrected for the lattice diamagnetism. The magnetization M is normalized to its value M_{max} at the highest magnetic field.

Each of the two curves in figure 1 exhibits the following characteristic features. At low fields, M rises very rapidly with H . This fast rise is mainly due to the alignment of the magnetic moments of the ‘singles’ (isolated Eu^{2+} spins, with no significant exchange coupling to other spins). The initial fast rise of M is followed by a ‘ramp’ which ends near 33 kOe. This ramp is due to ‘pairs’ (two spins coupled by the dominant exchange constant J). Several MSTs can be discerned on this ramp, particularly for $x = 0.011$. Between 33 and 50 kOe there is another, smaller, ramp. It corresponds to the completion of the alignment of the magnetic moments of the ‘triplets’ (three spins coupled by J). Above 50 kOe there is a slower rise of the magnetization due to the continuing alignment of spin clusters larger than triplets. Such large spin clusters (e.g., quartets, with four spins) are more numerous for the higher- x sample. For $x = 0.011$ the magnetization saturates before the highest field is reached. However, for $x = 0.042$ even at the highest field the magnetization is still rising very slowly because the magnetic moments of a few large spin clusters are still not fully aligned.

Figure 2 shows the derivative of the normalized magnetization $m = M/M_{max}$ with respect to H . The six large peaks for each sample, between 9 and 33 kOe, correspond to the second to seventh MSTs from pairs. The first MST from pairs, near 4.7 kOe, manifests itself as a shoulder

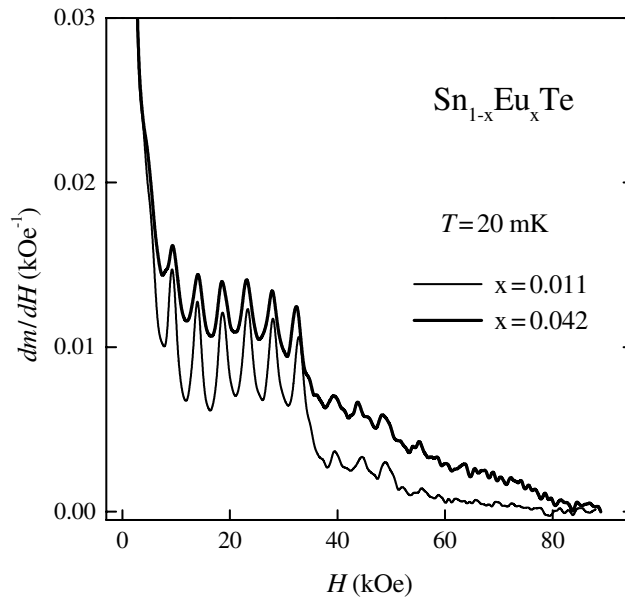


Figure 2. The numerical derivatives of the magnetization curves in figure 1.

on the fast drop of the derivative dm/dH at low H . (The drop of the derivative corresponds to the end of the initial fast rise of M . The shoulder associated with the first MST can be seen more clearly in an expanded view of the low-field data.) The three small peaks between 39.5 and 49 kOe are the last three MSTs from the triplets. The spacing between these three small peaks is the same as between the six large peaks, indicating that the exchange constant J for pairs and triplets is the same, as expected.

The fields H_n where the seven MSTs from pairs occur are related to the exchange constant J by the equation [4]

$$g\mu_B H_n = 2|J|n + \Delta_n \quad (1)$$

where $n = 1, 2, \dots, 7$ is the step number, and μ_B is the Bohr magneton. The parameter Δ_n accounts for possible shifts in the step positions due to smaller exchange constants not included in the model. In the present case it is very small and is approximated by a constant Δ , independent of n . Equation (1) is based on the Hamiltonian $-2J\mathbf{S}_1 \cdot \mathbf{S}_2$ for the exchange coupling between two spins. Figure 3 is a plot of the observed H_n (from the peaks in dm/dH) as a function of n . Clearly, equation (1) is well satisfied. The difference between the two values of J obtained from fits of the results on the two samples to this equation is only 2%. The average is $J/k_B = -0.311 \pm 0.006$ K, where k_B is the Boltzmann constant, and the uncertainty includes all known sources of error. The value for J corresponds to a separation of 4.66 kOe between adjacent MSTs. The experimental value for the shift Δ in equation (1) is negligible compared to $2|J|$. Our result for J is more accurate than the estimate $J/k_B \cong -0.5$ K obtained by Anderson *et al* [3] from the magnetization at 4.2 K.

It is known that the magnetic properties of the Eu chalcogenides (EuX, X = S, Se, Te) are governed by two exchange constants, for exchange between the first and second neighbours [15]. However, as discussed in our earlier works [4–6] on lead salts containing a small concentration of Eu ions, $\text{Pb}_{1-x}\text{Eu}_x\text{X}$, a single exchange constant dominates the exchange interactions. This is also the case for the present material, $\text{Sn}_{1-x}\text{Eu}_x\text{Te}$. The arguments are as

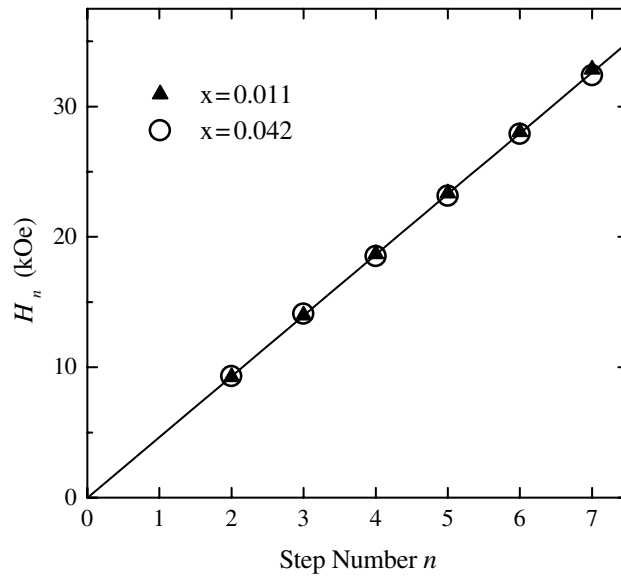


Figure 3. The fields H_n at the MSTs from pairs as a function of step number n . The straight line is a fit of all the data (for both samples) to equation (1).

follows. No additional series of steps, or ramps, indicating any other AF exchange constant have been observed, either in our data or in the high-field (23 T) magnetization measurements of Anderson *et al* [3]. Any other AF exchange constant should, then, be at least an order of magnitude smaller or larger than the present J . The Curie–Weiss temperatures obtained in the present work, however, rule out the existence of such large exchange constants, either AF or ferromagnetic. The exchange constant J measured in the present work is, therefore, the dominant exchange constant for $\text{Sn}_{1-x}\text{Eu}_x\text{Te}$. The identity of J cannot be firmly established from the present measurements. However, on the basis of the results on the $\text{Pb}_{1-x}\text{Eu}_x\text{X}$ series [4–6] we expect that it is the NN exchange constant.

The shape of a magnetization curve of a DMS at low temperatures is governed by the exchange constant J and by the probabilities of finding singles, pairs, triplets, etc. A larger probability of finding pairs, for example, will result in a larger ramp due to pairs. The various probabilities depend on the distribution of the Eu ions in the crystal. As a result, the shape of the magnetization curve depends on the distribution of the Eu ions.

Often one assumes a random distribution of the Eu ions over the cation sites. Simulations of the magnetization curves based on the cluster model can be done quite accurately, for low values of x , as described in reference [5]. Figure 4 shows the experimental curve for $x = 0.011$ and two numerical simulations[†]. The simulation labelled as $x_L = 0.011$ assumes a random distribution of the Eu ions in this crystal. It also assumes that J corresponds to the NN exchange constant. This simulation gives a very poor account of the experimental curve. The experimentally observed fast rise of M at low H is much smaller than in this simulation. Since the fast rise at low H is due to singles, the actual number of singles must be significantly lower than the number of singles predicted from a random distribution. On the other hand,

[†] The observed broadening of the MSTs at 20 mK is larger than the thermal broadening alone. For this reason the simulations, which include thermal broadening only, were carried out for $T = 100$ mK. The higher temperature in the simulations smooths sharp features, but has no effect on the magnitudes of the initial fast rise of M , or on the magnitudes of the ramps from pairs and triplets.

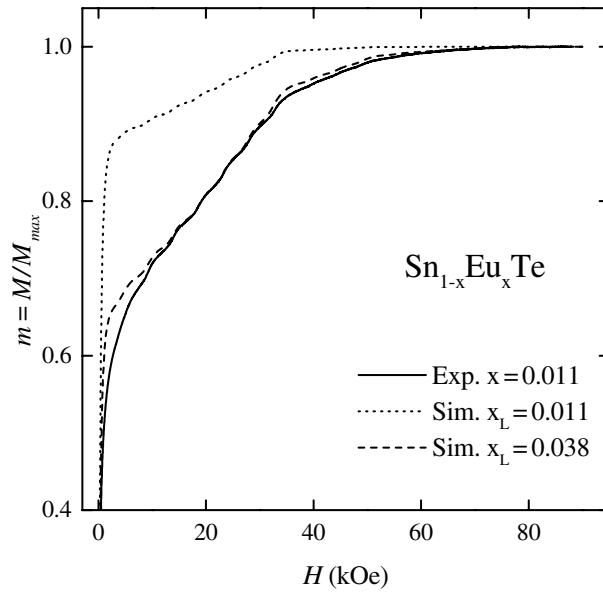


Figure 4. Comparison between the experimental 20 mK magnetization curve for $x = 0.011$ and numerical simulations based on two values of the local concentration x_L (see the first footnote in section 3). The simulations assume that J is the NN exchange constant.

the observed sizes of the ramps from pairs and triplets are much larger than in the simulation with $x_L = 0.011$, indicating that the actual numbers of pairs and triplets are much larger than calculated from a random distribution. If one retains the assumption of a random distribution but assumes that J is the next-nearest-neighbour (NNN) exchange constant, instead of the NN one, the agreement of the simulation with experiment becomes worse. These discrepancies between the data and simulations based on a random distribution cannot be explained by the small variation of x observed with the microprobe. The microprobe measures the Eu concentration on a length scale of $1 \mu\text{m}$. On this length scale the Eu distribution in this sample is homogeneous to within $\pm 10\%$. The magnetization curve, on the other hand, can be affected by concentration variations on a smaller length scale.

Because the actual number of singles is smaller than given by a random distribution, but the numbers of pairs and triplets are larger, the Eu ions must bunch together on a length scale smaller than $1 \mu\text{m}$. Most Eu ions are then in regions where the probability of finding a Eu ion on a nearby cation site is higher than the probability x for a random distribution over all cation sites in the crystal. The tendency of the Eu ions in $\text{Sn}_{1-x}\text{Eu}_x\text{Te}$ to bunch together is not unexpected in view of the observations of EuTe precipitates in many crystals.

For a random distribution the probability that a spin is in a particular type of cluster is a known function of x [16, 17]. For example, for an fcc cation lattice, and assuming that J is the NN exchange constant, the probability P_1 that a spin is a single is

$$P_1 = (1 - x)^{12}. \quad (2)$$

Equation (2) is not valid when the Eu spins bunch together, but the actual probability P_1 (the fraction of all spins which have no NNs) still governs the size of the fast rise of M at low H . One may then define an effective Eu concentration x_1 (relevant for singles) such that when x in equation (2) is replaced by x_1 it gives the actual value of P_1 . As the tendency of the Eu ions to aggregate increases, the value of x_1 increases.

An effective concentration x_2 , relevant for pairs, can be defined in a similar way. For a random distribution the probability that a spin is in a NN pair is

$$P_2 = 12x(1-x)^{18}. \quad (3)$$

When the spins bunch together, P_2 is no longer given by equation (3). The value of x_2 is then chosen in such a way that when x in equation (3) is replaced by x_2 it reproduces the actual value of P_2 . Other effective concentrations x_i can be defined for other cluster types†.

In general, the effective concentrations x_i depend on cluster type. However, for each of the present two samples the values of the x_i for singles, pairs, and triplets are close to each other. We therefore use a simplified phenomenological approach, introduced in reference [5], with a single local Eu concentration x_L , governing all cluster probabilities. For a given sample, simulations of the magnetization curve are carried out by computing the cluster probabilities with the equations for random distribution, but with the parameter x_L replacing the actual concentration x . The value of x_L is chosen to give the best agreement between the simulation and the data. In this simplified approach the ratio x_L/x quantifies the tendency of the Eu ions to bunch together.

Figure 4 shows two simulations for the sample with $x = 0.011$. The simulation with $x_L = x$ (i.e., random distribution) was discussed earlier. The simulation with $x_L = 0.038$ is the optimal simulation. The fact that this optimal simulation is quite close to the experimental curve justifies the approach based on x_L for this particular sample. The ratio obtained, $x_L/x \approx 3$, indicates a very strong tendency of the Eu ions to bunch together.

Simulations of the magnetization curve for the sample with $x = 0.042$ (not shown) resulted in $x_L = 0.08$. The quality of the agreement between the optimal simulation and the experimental curve is similar to that in figure 4. The ratio $x_L/x \approx 2$ shows that also in this sample the Eu ions have a strong tendency to bunch together.

Thus, for both samples the approach based on the local concentration x_L is quite successful in describing the actual cluster populations. As compared to the case of $\text{Pb}_{1-x}\text{Eu}_x\text{Te}$, for which $x_L/x \approx 1.4$ [5], the tendency for the Eu ions to bunch together in $\text{Sn}_{1-x}\text{Eu}_x\text{Te}$ is much stronger.

Acknowledgments

We are grateful to Professor R Fourcade for the x-ray measurements and to C Merlet for assistance in the microprobe measurements. The work in Brazil was supported by FAPESP, CNPq, and FINEP. The work in Poland was supported by the Polish Committee for Scientific Research.

References

- [1] Gorska M, Anderson J R, Kido G and Golacki Z 1990 *Solid State Commun.* **75** 363
- [2] Anderson J R, Kido G, Nishina Y, Gorska M, Kowalczyk L and Golacki Z 1990 *Phys. Rev. B* **41** 1014
- [3] Anderson J R, Gorska M, Oka Y, Jen J Y, Mogi I and Golacki Z 1995 *Solid State Commun.* **96** 11
- [4] Bindilatti V, Oliveira N F Jr, Shapira Y, McCabe G H, Liu M T, Isber S, Charar S, Averous M, McNiff E J Jr and Golacki Z 1996 *Phys. Rev. B* **53** 5472
- [5] ter Haar E, Bindilatti V, Oliveira N F Jr, McCabe G H, Shapira Y, Golacki Z, Charar S, Averous M and McNiff E J Jr 1997 *Phys. Rev. B* **56** 8912
- [6] Bindilatti V, ter Haar E, Oliveira N F Jr, Liu M T, Shapira Y, Gratens X, Charar S, Isber S, Masri P, Averous M, McNiff E J Jr and Golacki Z 1998 *Phys. Rev. B* **57** 7854

† Except for x_1 , each of the effective concentrations x_i can be assigned two values, because each function $P_i(x)$ has a maximum. However, this ambiguity is of no consequence for the present analysis, because a single effective concentration x_L is required to lead to reasonable approximations for all probabilities which significantly affect the magnetization curve. The unique value of x_1 removes any large uncertainty in x_L .

- [7] Shapira Y 1990 *J. Appl. Phys.* **67** 5090
- [8] Gorska M, Anderson J R, Peng J L and Golacki Z 1995 *J. Phys. Chem. Solids* **56** 1253
- [9] Golacki Z and Heinonen M 1997 *Acta Phys. Pol. A* **91** 775
- [10] Urgan P and Sperlich G 1972 *Phys. Lett. A* **42** 117
- [11] Gratens X and Errebbahi A 1998 unpublished
- [12] Gaj J A, Planel R and Fishman G 1979 *Solid State Commun.* **29** 435
- [13] Bindilatti V and Oliveira N F Jr 1994 *Physica B* **194–196** 37
- [14] ter Haar E, Wagner R, van Woerkens C M C M, Steel S C, Frossati G, Skrbek L, Meisel M W, Bindilatti V, Rodrigues A R, Martin R V and Oliveira N F Jr 1995 *J. Low Temp. Phys.* 151
- [15] Mauger A and Godart C 1986 *Phys. Rep.* **141** 51
- [16] Behringer R E 1957 *J. Chem. Phys.* **26** 1504
- [17] Liu M T, Shapira Y, ter Haar E, Bindilatti V and McNiff E J Jr 1996 *Phys. Rev. B* **54** 6457